Diabetic Complications Consortium

Application Title: Role of gut extracellular vesicles in the development of diabetic peripheral neuropathy

Principal Investigator: Liu, Xianshuang

1. Project Accomplishments:

The mechanisms by which gut micorbiota dysbiosis induced by diabetes contributes to the diabetic complication including diabetic peripheral neuropathy (DPN) remain unclear. Within the funding year, we demonstrate that administration of gut microbiota-derived extracellular vesicles (gut-EVs) from diabetic mice (db-gut-EVs) to non-diabetic mice induced DPN, whereas administration of EVs derived from Lactobacillus probiotic (probiotic-EVs) to diabetic mice with DPN significantly alleviated the inflammatory response and promoted sensory and motor recovery in diabetic mice with peripheral neuropathy. Mechanistically, we found that db-gut-EVs and probiotic-EVs activated and suppressed, respectively, proinflammatory monocytes/macrophages, leading to exacerbate or to alleviate DPN. Toll like receptor 4 (TLR4) mediated db-gut-EVs induced proinflammatory monocytes/macropahges. All together, our study provides new mechanistic insights into gut-EVs in mediating the gut microbiota-peripheral nerve communication under DPN. Additionally, our finding suggests that the probiotic-EVs have a therapeutic potential for treatment of DPN.

Specific Aims and Results:

For each specific aim provide the data (includes figures and tables) and progress in each aim.

The specific aims remain unchanged. We have performed the following experiments.

Specific Aim 1: To test the hypothesis that db-gut-EVs promote the progression of DPN.

Characterization of db-gut-EVs from diabetic mice with DPN:

Using differential ultracentrifugation method, we isolated the gut-EVs from male mouse stool samples. Transmission electron microscopy (TEM) and Nanosight confirmed these EVs had a mean size ~150 nm **(Fig. 1A, B)**. Analysis of these EVs with 16S rRNA sequencing revealed that gut-EVs contained composition of bacterial species, indicating that these EVs were microbiota-derived EVs **(Fig. 1C)**. Compared to dm-gut-EVs, taxa analysis using LEfSe algorithm showed that db-gut-EVs from diabetic db mice aged 20 weeks displayed a significantly altered composition of micobiota **(Fig. 1C)**. In addition, two types of gut-EVs showed a marked separation on a principal coordinate analysis (PCoA) based on Bray-Curtis distance matrices **(Fig. 1D)**. These data suggest that the different bacteria-derived EV composition of dm- and db-gut-EVs may have differential effects on DPN.

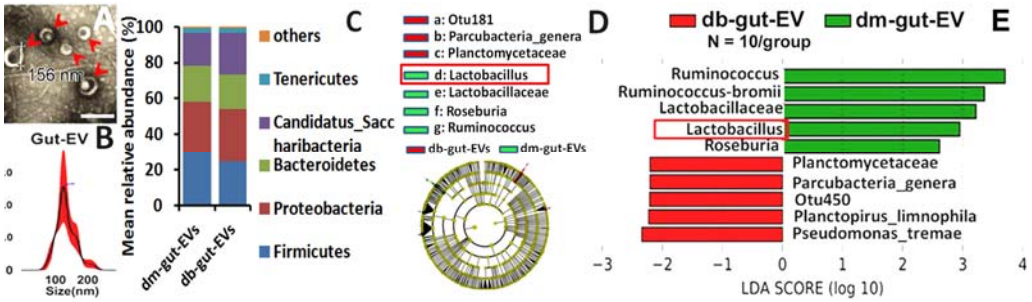

Fig 1. A: A representative image of gut-EVs from stools of db mice analyzed by transmission electron microscopy (TEM, red arrows). Bar: 200nm. **B:** Size distribution of gut-EVs. Differences in OTU abundance at phyla level **(C)**, Shannon diversity index **(D)** and taxa abundance bars at the genus level **(E)** of microbiota composition in gut-EVs from diabetic db (db-gut-EVs) and non-diabetic dm (dm-gut-EVs) mice using 16s rRNA gene sequencing**.**

Bio-distribution of bacterial EVs:

We isolated the bacterial EVs from E. coli carrying CD63-GFP fluorescent reporter (SBI), a marker of EVs, and fed normal mice by oral gavage ($1x10^{10}$ particles/injection) once a day for 3 consecutive days.

Using EV capture beads (SBI) in combined with flow cytometry, we detected the GFP signaling (11%) in the sera of mice fed with CD63-GFP labeled EVs **(Fig. 2A)**, nevertheless CD63-GFP signaling was not detected in sera from the mice fed with EVs carrying empty vector **(Fig. 2B)**. We also observed the coexpression of CD63-GFP labeled EVs within F4/80$^+$ macrophages **(Fig. 3A)** and NF200$^+$ peripheral nerves **(Fig. 3B)** of sciatic nerves tissues**,** suggesting that bacterial EVs can travel from the gut to circulation and be internalized by monocytes/macrophages and distal peripheral nerves, thereby mediating the gut-peripheral nerve communication.

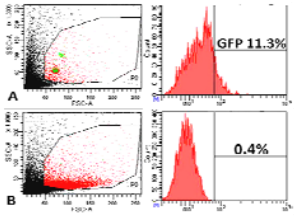

Fig 2. Quantification of GFP-labeling bacteria-derived EVs in the sera by FCM **(A, B)** from mice fed with bacterial EVs from E.Coli carrying CD63-GFP **(A)** and control mice **(B)**.

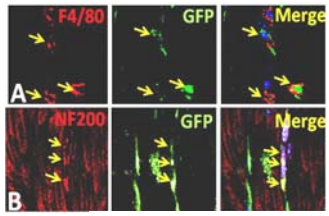

Fig 3. Localization of bacterial CD63-GFP$^+$ EVs (green) in F4/80$^+$ macrophages (**A**, red) and NF200+ neurons (**B**, red) of sciatic nerve from db mice fed with bacterial EVs carrying CD63-GFP.

Db-gut-EVs promote the progression of DPN:

Db-gut-EVs (1x10^{10} particles/injection) were administered to male diabetic db mice at the age of 7 weeks via a tail vein twice a week for 10 weeks. We found that diabetic mice treated with db-gut-EVs exhibited significant impairments of thermal response measured by the plantar test and mechanical sensitivity evaluated by the Von Frey test compared to non-diabetic dm mice at the age of 11-12

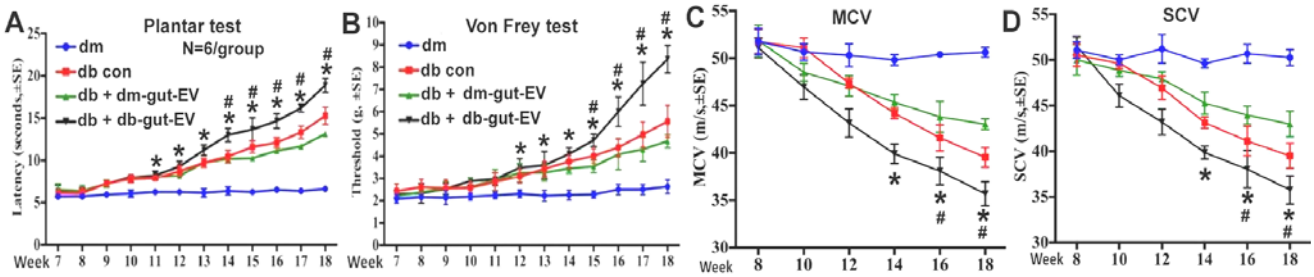

Fig 4. Panels show increased thermal and mechanical response latencies measured by plantar test **(A)** and Von Frey test **(B)**, respectively, as well as impaired MCV **(C)** and SCV **(D)** in diabetic db mice treated with db- or dm-gut-EVs. ***p<0.05**, db con, db + dm-gut-EV, db + db-gut-EV vs dm; **#** p<0.05 db + db-gut-EV vs db con.

weeks. A more severe impairment of thermal and mechanical response was evident in diabetic mice treated with db-gut-EVs, compared to diabetic mice treated with control dm-gut-EVs and diabetic mice alone at age of 15 weeks **(Fig. 4A, B)**. Electrophysiological recording showed that diabetic mice treated with db-gut-EVs displayed a significant reduction of the motor (MCV) and sensory (SCV) compared to non-diabetic mice at the age of 14 weeks. Impairment of SCV and MCV was more severe in diabetic mice treated with db-gut-EVs compared to diabetic mice treated with control dm-gut-EVs and diabetic mice alone at the age of 16 weeks **(Fig. 4C, D)**. These data suggest that db-gut-EVs promote the development of DPN. Neither of the gut-EV treatments significantly affected the blood levels of glucose and lipids and animal body weight of db mice (**Table 1**). These data indicate that db-gut-EVs worsen diabetes-induced peripheral nerve damage in a glucose metabolism-independent manner.

Table 1. Effect of gut-EVs on glucose, lipids and body weight

	dm+saline	db+saline	db+dm-gut-EVs	db+db-gut-EVs
Body Weight (g)	33.0±1.8	54.5±7.8***	52.8±5.3***	55.2±8.3***
Glucose (mmol/L)	7.2±0.5	22.4±3.2***	21.5±1.9***	23.0±6.2***
A1C (%)	4.0±0.2	10.3±2.1***	10.0±1.1***	10.0±1.1***
TC (mmol/L)	2.3±0.3	4.4±0.1***	4.5±0.6***	4.5±0.4***
TG (mmol/L)	0.5±0.1	1.2±0.2***	1.1±0.4***	1.2±0.4***
Insulin(ng/ml)	0.8±0.2	2.1±0.3***	2.2±0.2***	2.0±0.2***

Values are mean ± SD. N=10/group. ***p<0.001, vs dm+saline

Db-gut-EVs affect the neurite outgrowth in vitro:

We assessed the effect of gut-EVs on neurite outgrowth of DRG neurons. Primary cultured adult DRG neurons were exposed to db-gut-EVs (10^8particles/ml) for 48hrs. We found that DRG neurons exhibited impaired neurite outgrowth stained with antibody against Tuj1 in the presence of db-gut-EVs, compared with the neurons treated with control solution **(Fig. 5).** These data suggest that db-gut-EVs result in the sensory neuron damage.

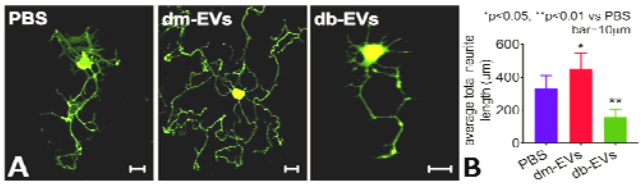

Fig 5. Db-gut-EVs inhibit outgrowth of the neurites of the DRG neurons from the diabetic animals.

Db-gut-EVs induce the neuroinflammatory response via TLR4:

Diabetes can induce inflammatory response of monocytes/macrophages in circulation and peripheral nerves, and suppression of this inflammation improves functional recovery of DPN. However, the mechanism underlying diabetes-induced neuroinflammation have not been fully understood. To test if db-gut-EVs stimulated the immune response, inflammatory cytokines were analyzed in animals as outlined above. Our data showed that db-gut-EVs significantly elevated levels of pro-inflammatory cytokines (TNFα, IL-1β and IL-6) assayed by ELISA in both sera and sciatic nerve tissues **(Fig. 6A, B),** compared to dm-gut-EVs and saline. Also, TLR4 levels were significantly increased and reduced in sciatic nerves of db mice treated with db-gut-EVs and dm-gut-EVs, respectively **(Fig. 6C, D).** Upregulation of TLR4 in monocytes has been reported in patients with DPN. The results suggest that the TLR4 signaling pathway mediates db-gut-EV-induced activation of monocytes/macropahges, which is clinically relevant.

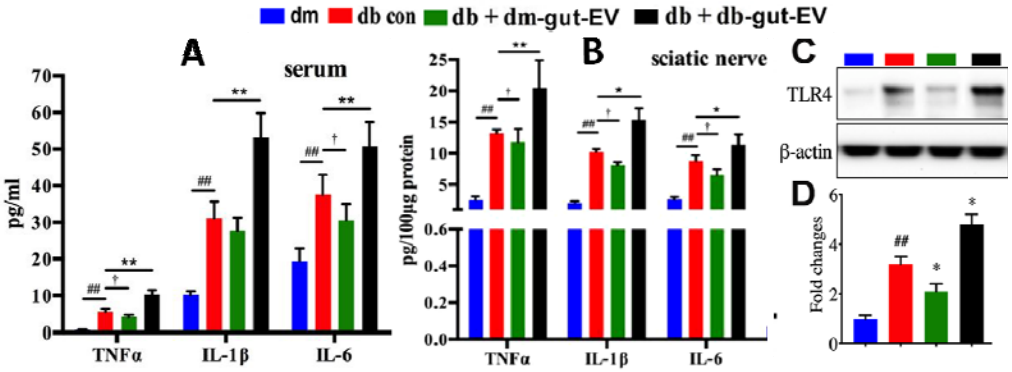

Fig 6. ELISA analysis of cytokines in sciatic nerve tissues **(A)** and the sera **(B)** as well as Western blot analysis of TLR4 in sciatic nerve tissues **(C, D)** of mice treated with db- and dm-gut-EVs.

Conditional knockdown of TLR4 in monocytes/macropahges alleviates the inflammatory response and suppresses peripheral nerve injury induced by db-gut-EVs:

To further investigate the role of TLR4 in DPN, we mated *Lyz2-CreER^{T2}* with *TLR4$^{flox/flox}$* **(Fig 7,** Jackson Lab**)** and produced *Lyz2-CreER^{T2};TLR4$^{-/-}$* transgenic mouse lines in which TLR4 was specifically ablated in monocytes/macropahges after tamoxifen administration. Treatment of WT mice with db-gut-EVs ($1x10^{10}$ particles/injection) via tail vein twice per week for 8 weeks significantly increased the levels of pro-inflammatory cytokines (TNFα and IL-1β) assayed by ELISA in both sera and sciatic nerve tissues **(Fig. 8),** compared to WT mice treated with normal saline. However, upregulated pro-inflammatory cytokines were significantly reduced in TLR4 KO mice compared with WT mice treated with db-gut-EVs **(Fig. 8).**

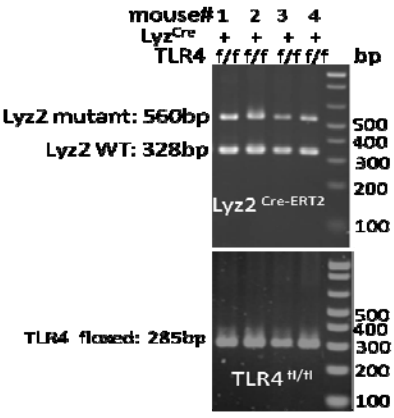

Fig 7. PCR products of tail DNA identify the presence of Cre recombinase in *Lyz2-CreER^{T2}* and floxed TLR4 in *TLR4$^{flox/flox}$* mouse line. (f/f:flox/flox, WT: wild type).

Moreover, we observed that administration of db-gut-EVs significantly reduced thermal response latencies **(Fig. 9A)** and reduced SCV **(Fig. 9B)** at 8 weeks post-treatment in WT mice, which are consistent with the data outlined in **Fig 4**. However, the thermal response latencies

and SCV were improved in monocyte TLR4 KO mice compared to WT mice treated with db-gut-EVs **(Fig. 9).** These data suggest that deletion of TLR4 reduces db-gut-EV-induced neuroinflammation and alleviates peripheral nerve damage. Therefore, TLR4 mediates the interaction between db-gut-EVs and peripheral nerves.

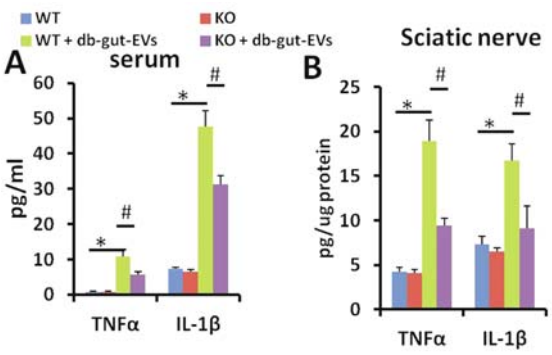

Fig 8. ELISA analysis of cytokines in the sera **(A)** and sciatic nerve tissues **(B)** of *Lyz2-CreER^{T2};TLR4$^{-/-}$* or WT mice treated with db-gut-EVs. N=3/group, *P<0.05 vs WT, #P<0.05 vs WT + db-gut-EV treatment.

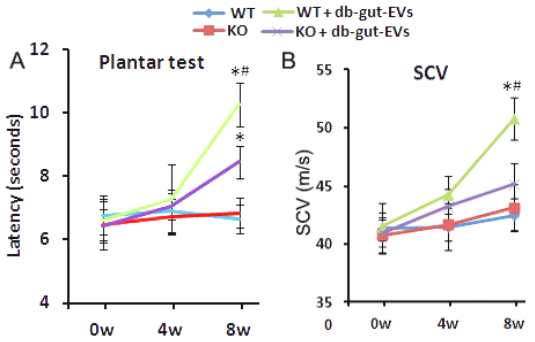

Fig 8. Panels show the thermal response latency measured by plantar test **(A)** and SCV **(B)** in TLR4 KO or WT mice treated with db-gut-EVs, respectively. N=5/group. *p<0.05 vs WT, #p<0.05, KO + db-gut-EVs vs WT + db-gut-EVs.

Specific Aim 2: To test the hypothesis that probiotic-EVs alleviate DPN.

Treatment with probiotic-EVs improves neurological outcomes in diabetic mice:

Our 16S rRNA sequencing showed a significantly reduced composition of probiotic-EVs such as Lactobacillus **(Fig. 1C).** To investigate its effect on DPN, probiotic-EVs were isolated from culture media of Lactobacillus (Lacto-EVs, 14869, ATCC) and characterized by TEM and Nanosight **(Fig. 10A, B)**. Db mice aged 20 weeks were treated with Lacto-EVs (1×10^{10} particles/injection) twice a week for 12 consecutive weeks. We found that compared to saline control, Lacto-EVs significantly reduced thermal response latencies **(Fig. 10C, D)** and improved SCV and MCS at 8 weeks post-treatment **(Fig. 10E, F)**.

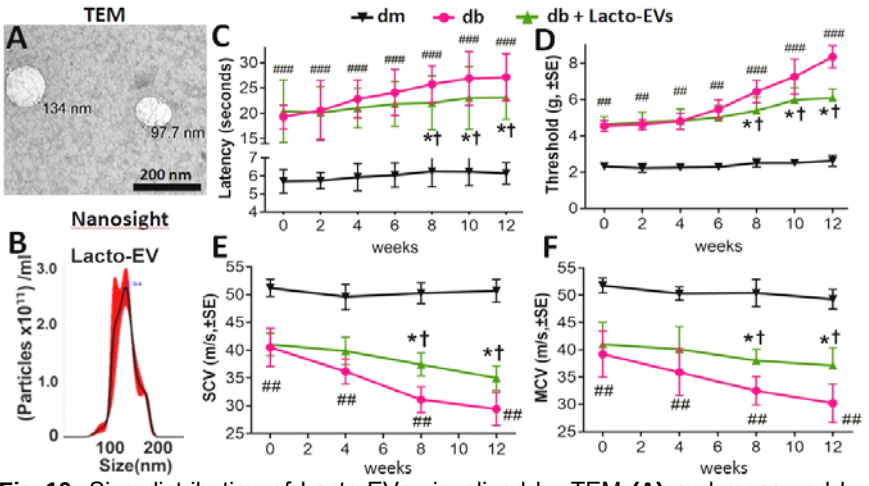

Fig 10. Size distribution of Lacto-EVs visualized by TEM **(A)** and measured by Nanosight **(B)**. Treatment with Lacto-EVs significantly improved neurological function measured by radial heat plate test **(C),** Von Frey test **(D),** SCV **(E)** and MCV **(F)** in db mice, compared to db mice alone. N=6/group. ###p<0.001 db vs dm; *p<0.05, db + Lacto-EVs vs db; † p<0.05 db + Lacto-EVs vs dm.

Treatment with probiotics-EVs promotes small nerve fiber reinnervation:

Intraepidermal *nerve* fiber (IENF) density measurement on patient skin biopsy has been widely used in the diagnosis of peripheral neuropathy and in monitoring its response to treatment in clinics. We found that compared to age-matched non-diabetic dm mice, db mice showed approximately 50% decrease in the number of IENF in skin of the foot-pads assayed by the number of protein gene product 9.5 (PGP9.5^{+}) fibers **(Fig. 11)**, which expressed in all types of efferent and afferent peripheral nerve fibers[78]. In contrast, treatment with Lacto-EVs significantly suppressed diabetes-reduced IENF compared to the db mice (**Fig. 11)**. Our data suggest that treatment with the probiotics-EVs improve peripheral nerve function and neurological outcomes in diabetic mice.

Probiotic-EVs promote the neurite outgrowth:

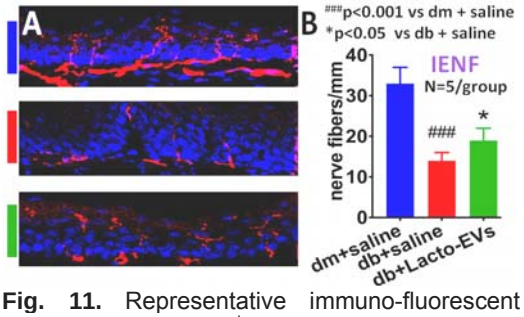

Fig. 11. Representative immuno-fluorescent images show PGP9.5^{+} IENFs (green, arrows, **A**) in diabetic db mice treated with Lacto-EVs. Panel **B** shows quantitative data of IENFs. Bar=50μm.

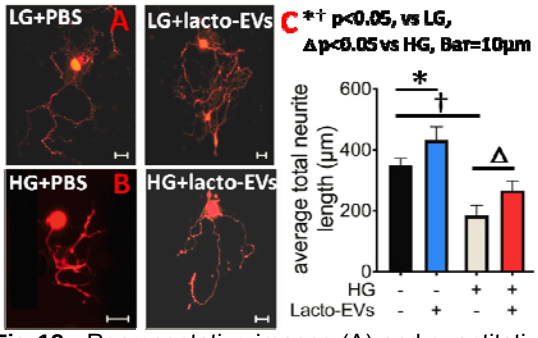

Fig 12. Representative images (A) and quantitative data **(E)** of Tuj1^{+} neurite length of adult DRG neurons treated with Lacto-EVs under LG or HG media.

Our data showed that sensory neurons treated with Lacto-EVs displayed a significant improvement in neurite regeneration of DRG neurons in high glucose (HG) media compared with those treated with PBS solution under normal (LG) or HG condition **(Fig. 12).** Our data suggest that probiotic-EV treatment reduces peripheral nerve damage induced by diabetes.

Probiotic-EVs alleviate the proinflammatory response in systemic and sciatic nerves:

Inflammation occurs early in the development of diabetes and targets both nerve fibers to result in the peripheral nerve dysfunction characteristic of DPN. Our data showed that the population of CD45^{+}Ly6C^{high} inflammatory monocytes/macrophages assayed by FACS **(Fig. 13)** and circulating proinflammatory cytokines assayed with ELISA were significantly upregulated in the sera (**Fig. 14A)** and sciatic nerve tissues **(Fig. 14B)** of db mice compared to dm mice. Administration of Lacto-EVs significantly reduced the population of CD45^{+}Ly6C^{high} inflammatory monocyte/macrophage population **(Fig. 13)** and levels of proinflammatory cytokines in the sera (**Fig. 13)** of db mice, compared to db alone mice, indicating probiotics-EVs modulate the innate immune response related to DPN. These data suggest that administration of probiotic-EVs suppress the progression of DPN through inhibiting the inflammatory response.

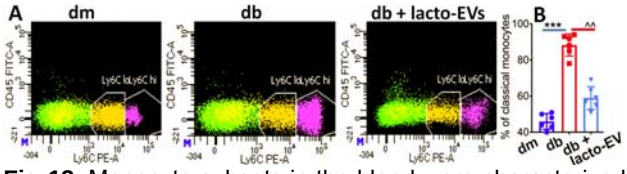

Fig 13. Monocyte subsets in the blood were characterized by CD45/FITC and Ly6C/PE staining. **A**: Representative pattern plot of CD45^{+}Ly6C^{high} inflammatory monocyte subsets in the peripheral blood of db mice treated with Lacto-EVs compared with db and dm mice. Red: Ly6c^{hi}, yellow: Ly6c^{low}.**B:** Quantification of CD45^{+}Ly6C^{high} inflammatory monocyte subsets. N=6/group. ***P<0.001 vs dm; ^^p<0.01 vs db.

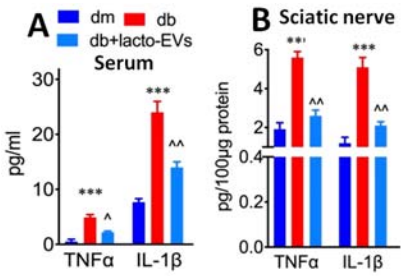

Fig 14. Analysis of proinflammatory cytokines assayed by ELISA in sera **(A)** and sciatic nerve tissues **(B)** in db mice alone or mice treated with Lacto-EVs**.** N=6/group. ***P<0.001 vs dm; ^ p<0.05, ^^p<0.01 vs db.

2. Publications:

Please list any publications resulting from the project.

In preparation.